A DFT Study on the Mechanism of Palladium-Catalyzed Alkyne Hydrogenation: Neutral versus Cationic Pathways

Joaquín López-Serrano,[†] Agustí Lledós,*[,‡] and Simon B. Duckett*[,†]

Department of Chemistry, University of York, Heslington, YO10 5DD, York, United Kingdom, and Departament de Química, Universitat Autònoma de Barcelona, 08193 Barcelona, Spain

Received March 29, 2007

A DFT study on the palladium-bisphosphine-catalyzed hydrogenation of alkynes is presented. The theoretical study explores the feasibility of two independent mechanisms, one based on the neutral species $Pd(0)(P_2)$ (where $P_2 = 2PH_3$ or $PH_2CH_2CH_2PH_2$) and the second based on cationic intermediates of the type $[Pd(II)(P_2)(H)]^+$. The paper compares the theoretical results with experimental observations obtained in a parallel NMR study. The calculations reveal that for the Pd(0) system to achieve useful catalysis a phosphine loss mechanism is necessary with subsequent binding of the alkyne to $Pd(P_2)$ being followed by phosphine loss and H_2 coordination. After hydride transfer, the formation of $Pd(PH_3)(H)(CH{=}CH_2)$ is predicted. This species is instrumental in forming $Pd(P_2)(\eta^2\text{-}CH_2{=}CH_2)$. Formation of $Pd(P_2)(H)(CH_2CH_3)$ also proceeds via phosphine loss, in this case from $Pd(P_2)(\eta^2\text{-}CH_2{=}CH_2)$. In contrast, the cationic mechanism involves $Pd(II)(P_2)(H)^+$, which reacts with the alkyne to form $Pd(P_2)(CH{=}CH_2)^+$ directly. A role for $Pd(P_2)(H)(\eta^2\text{-}CH_2{=}CH_2)^+$ and $Pd(P_2)(CH_2CH_3)^+$ in both alkene isomerization and hydrogenation is established. For the cationic cycle, alkene isomerization is predicted to be facile, while reductive elimination of alkane via H_2 coordination involves a higher barrier, in good agreement with experimental observations. For the neutral cycle, both alkene isomerization and alkane formation also involve alkylpalladium species such as $Pd(P_2)(H)(CH_2CH_3)$, but they now correspond to high-energy processes and are predicted to be less likely. Overall calculations support for the palladium-bisphosphine systems a reaction mechanism based on cationic monohydride precursors.

Introduction

Palladium complexes are among the most extensively used in catalysis. They are best known for their excellent performance in C−C (and C−heteroatom) bond forming reactions and are utilized as a versatile synthetic tool in many research laboratories. Less explored, however, is their ability to catalyze reduction, oxidation, isomerization, and carbonylation reactions[1] including the industrially significant hydroformylation of alkenes.[2] Although it has been accepted that many of these reactions can involve palladium hydride complexes as key intermediates, their detection is relatively rare.[3,4] It is even more difficult to prove a direct role for such hydride complexes in the ensuing transformation and thereby distinguish a true catalytic intermediate from a thermodynamic sink that actually reduces overall catalytic activity.

A reaction catalyzed by palladium complexes that has received much less attention is the semihydrogenation of alkynes. A number of catalysts are able to undertake the selective reduction of alkynes into *cis*-alkenes, with the heterogeneous Lindlar catalyst being the most well-known.[5,6] Related homogeneous catalysts include palladium(0) diimine complexes such as those recently described by Elsevier.[7] Here we present a theoretical study[8,9] of alkyne semihydrogenation that developed in parallel with a *para*-hydrogen-based NMR investigation,[10–12] the results of which have already been reported.[13–15]

In these experimental studies, palladium complexes of the type $Pd(P_2)(OTf)_2$ [where $P_2 = 2PEt_3$ or the bidentate chelating phosphines bcope, $(C_8H_{14})PCH_2CH_2P(C_8H_{14})$, and ^{t}bucope, $(C_8H_{14})PC_6H_4CH_2P(^tBu)_2$] were used as precatalysts for the hydrogenation of diphenylacetylene and 1-phenylpropyne.[13–15] The main organic products detected in these reactions proved to be the corresponding *trans*-alkenes, and when a *cis*-alkene was used as the substrate, isomerization proved facile even though only relatively small amounts of the corresponding alkane were detected. In addition, a number of *para*-hydrogen-

* Corresponding authors. E-mail: sbd3@york.ac.uk; agusti@klingon.uab.es.
† University of York.
‡ Universitat Autònoma de Barcelona.

(1) Negishi, E.-I. *Handbook of Organopalladium Chemistry for Organic Synthesis*; Wiley: New York, 2002.
(2) Konya, D.; Almeida Leñero, K. Q.; Drent, E. *Organometallics* **2006**, *25*, 3166–3174.
(3) Clegg, W.; Eastham, G. R.; Elsegood, M. R. J.; Heaton, B. T.; Iggo, J. A.; Tooze, R. P.; Whyman, R.; Zacchini, S. *Dalton Trans.* **2002**, *3300*, 3308.
(4) Clegg, W.; Eastham, G. R.; Elsegood, M. R. J.; Heaton, B. T.; Iggo, J. A.; Tooze, R. P.; Whyman, R.; Zacchini, S. *Organometallics* **2002**, *21*, 1832–1840.
(5) Lindlar, H. *Helv. Chim. Acta* **1952**, *35*, 446–456.
(6) Lindlar, H.; Dubuis, R. *Org. Synth.* **1966**, *46*, 89.
(7) Kluwer, A. M.; Koblenz, T. S.; Jonischkeit, T.; Woelk, K.; Elsevier, C. J. *J. Am. Chem. Soc.* **2005**, *127*, 15470–15480.
(8) Niu, S.; Hall, M. B. *Chem. Rev.* **2000**, *100*, 353–405.
(9) Dedieu, A. *Chem. Rev.* **2000**, *100*, 543–600.
(10) Duckett, S. B.; Sleigh, C. J. *Prog. Nucl. Magn. Reson. Spectrosc.* **1999**, *34*, 71–93.
(11) Blazina, D.; Duckett, S. B.; Dunne, J. P.; Godard, C. *Dalton Trans.* **2004**, (17), 2601–2609.
(12) Canet, D.; Aroulanda, C.; Mutzenhardt, P.; Aime, S.; Gobetto, R.; Reineri, F. *Concepts Magn. Reson. Part A* **2006**, *28A* (5), 321–330.
(13) Dunne, J. P.; Aiken, S.; Duckett, S. B.; Konya, D.; Lenero, K. Q. A.; Drent, E. *J. Am. Chem. Soc.* **2004**, *126* (51), 16708–16709.
(14) López-Serrano, J.; Duckett, S. B.; Lledós, A. *J. Am. Chem. Soc.* **2006**, *128* (30), 9596–9597.
(15) López-Serrano, J.; Duckett, S. B.; Aiken, S.; Almeida Leñero, K. Q.; Drent, E.; Dunne, J. P.; Konya, D.; Whitwood, A. C. *J. Am. Chem. Soc.* **2007**, *129*, 6513–6527.

10.1021/om700307c CCC: $40.75
Publication on Web 12/08/2007

enhanced resonances were detected for a series of palladium complexes in these reactions. The species giving rise to these resonances were shown to participate directly in catalysis via appropriate magnetization transfer experiments. The original PHIP NMR data, however, only provided part of the information necessary to fully characterize these reaction products. This situation arose because while the PHIP technique yields a potential 31 000-fold signal enhancement,[16] it does so only for polarized hydrogen atoms originating from *para*-hydrogen. Other nuclei are usually detected indirectly, via the observation of scalar couplings (e.g., ^{1}H, ^{13}C, or ^{31}P), or directly, via magnetization transfer from the enhanced protons.[17,18] In view of the fact that the observation of these PHIP-enhanced species by conventional NMR methods would be unusual if they are true reaction intermediates because of their low concentrations, only limited NMR data were obtained. In this case, the key palladium-based intermediates were described as containing two phosphine ligands and an alkyl of the type Pd(CHRCH$_2$R′). This deduction was based on the detection of PHIP-enhanced resonances for the alkyl protons of the associated species, with the corresponding ^{13}C and ^{31}P resonances being observed by cross-polarization experiments. Consequently, the detected species were deduced to either be cationic in nature or contain an additional hydride ligand.

When these reactions were completed in methanol, the detection of the alkyl-containing complexes [Pd(bcope)(CHPhCH$_2$Ph)](OTf) and [Pd(^{t}bucope)(CHPhCH$_2$Ph)](OTf), in addition to the vinyl-containing species [Pd(bcope)(CPh═CHPh)(MeOD)](OTf) and [Pd(^{t}bucope)(CPh═CHPh)(MeOD)](OTf), was proposed. It was only when pyridine was added to the solution, and new signals for the corresponding adducts [Pd(bcope)(CPh═CHPh)(pyridine)](OTf) and [Pd(^{t}bucope)(CPh═CHPh)(pyridine)](OTf) seen, that the cationic nature of these species was confirmed. The palladium hydrides [Pd(bcope)(H)(pyridine)](OTf), two isomers of [Pd(^{t}bucope)(H)(pyridine)](OTf), and the neutral complex [Pd(^{t}bucope)(H)$_2$] were also observed in this study.

This paper describes the results obtained from a DFT study that was completed in parallel to the experimental work with the aim of validating the solution-based observations. The DFT study employs monodentate phosphines, simulated by PH_3, as well as chelating phosphines based on dhpe ($PH_2CH_2CH_2PH_2$). The alkyne used in this study is acetylene. Results map appropriate transition states and associated energy barriers both in the gas phase and in methanol (via a polarizable continuum model (PCM)). Mechanisms involving neutral palladium intermediates are explicitly compared with those predicted for a reaction proceeding via a palladium monohydride cation.[19–21] These two schemes are indicated in Figure 1 with the associated NMR trace illustrating the PHIP effect seen in the ^{1}H resonances of the *cis*-alkene product.[22,23]

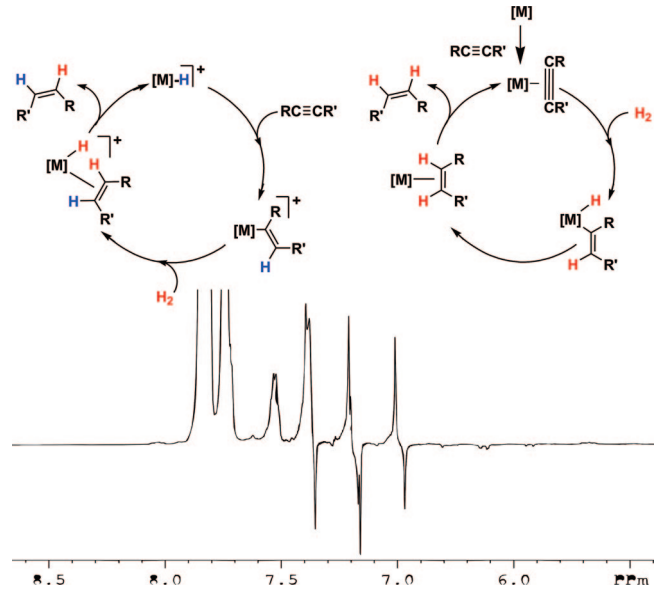

Figure 1. Schematic mechanisms for the palladium-catalyzed semihydrogenation of an alkyne via a cationic mechanism (left) and a neutral cycle (right). The colors serve to illustrate the role the hydrogen atoms play in the molecularity of the reaction. The NMR trace shows the PHIP-enhanced resonance (with ^{13}C satellites) seen for the CH═CH protons of *cis*-stilbene produced from mono-^{13}C-labeled diphenylacetylene in the parallel experimental study.

Computational Details

All calculations were performed using the GAUSSIAN 03 series of programs,[24] using the B3LYP functional.[25,26] The structures of the reactants, intermediates, transition states, and products were fully optimized in the gas phase without any symmetry restrictions using basis set 1 (BS1). In this basis set an effective core potential[27] and its associated double-ζ LANL2DZ[24,28] basis set were used for the palladium and phosphorus atoms. An extra series of d-polarization functions has also been added for P.[28] Hydride atoms and H atoms involved in hydrogenation processes were represented by means of the 6-31G(d,p) basis set, whereas for the rest of the H atoms the 6-31G basis set was used. C, N, and O atoms where represented by the 6-31G(d) basis set.[29–31] Frequency calculations were

(16) Anwar, M. S.; Blazina, D.; Carterer, H.; Duckett, S. B.; Halstead, T. K.; Jones, J. A.; Kozak, C. M.; Taylor, R. J. K. *Phys. Rev. Lett.* **2004**, *93*, 040501–040504.
(17) Duckett, S. B.; Newell, C. L.; Eisemberg, R. *J. Am. Chem. Soc.* **1993**, *115*, 1156–1157.
(18) Haake, M.; Natterer, J.; Bargon, J. *J. Am. Chem. Soc.* **1996**, *118*, 8688–8691.
(19) Eastham, G. R.; Tooze, R. P.; Kilner, M.; Foster, D. F.; Cole-Hamilton, D. J. *Dalton Trans.* **2002**, *1613*, 1617.
(20) Fairlamb, I. S. S.; Grant, S.; Tommasi, S.; Lynam, J. M.; Bandini, M.; Dong, H.; Lin, Z.; Whitwood, A. C. *Adv. Synth. Catal.* **2006**, *348*, 2515–2530.
(21) Bianchini, C.; Mantovani, G.; Meli, A.; Oberhauser, W.; Bruggeller, P.; Stampfl, T. *Dalton Trans.* **2001**, *690*, 698.
(22) Jang, M.; Duckett, S. B.; Eisemberg, R. *Organometallics* **1996**, *15*, 2863–2865.
(23) Millar, S. P.; Jang, M.; Lachicotte, R. J.; Eisemberg, R. *Inorg. Chim. Acta* **1998**, *270*, 363–375.
(24) Frisch, M. J.; Trucks, G. W.; Schlegel, H. B.; Scuseria, G. E.; Robb, M. A.; Cheeseman, J. R.; Montgomery, J. A., Jr.; Vreven, T.; Kudin, K. N.; Burant, J. C.; Millam, J. M.; Iyengar, S. S.; Tomasi, J.; Barone, V.; Mennucci, B.; Cossi, M.; Scalmani, G.; Rega, N.; Petersson, G. A.; Nakatsuji, H.; Hada, M.; Ehara, M.; Toyota, K.; Fukuda, R.; Hasegawa, J.; Ishida, M.; Nakajima, T.; Honda, Y.; Kitao, O.; Nakai, H.; Klene, M.; Li, X.; Knox, J. E.; Hratchian, H. P.; Cross, J. B.; Bakken, V.; Adamo, C.; Jaramillo, J.; Gomperts, R.; Stratmann, R. E.; Yazyev, O.; Austin, A. J.; Cammi, R.; Pomelli, C.; Ochterski, J. W.; Ayala, P. Y.; Morokuma, K.; Voth, G. A.; Salvador, P.; Dannenberg, J. J.; Zakrzewski, V. G.; Dapprich, S.; Daniels, A. D.; Strain, M. C.; Farkas, O.; Mallick, D. K.; Rabuck, A. D.; Raghavachari, K.; Foresman, J. B.; Ortiz, J. V.; Cui, Q.; Baboul, A. G.; Clifford, S.; Cioslowski, J.; Stefanov, B. B.; Liu, G.; Liashenko, A.; Piskorz, P.; Komaroni, I.; Martin, R. L.; Fox, D. J.; Keith, T.; Al-Laham, M. A.; Peng, C. Y.; Nanayakkara, A.; Challacombe, M.; Gill, P. M. W.; Johnson, B.; Chen, W.; Wong, M. W.; Gonzalez, C.; Pople, J. A. *Gaussian 03, Revision D.01*; Gaussian, Inc.: Wallingford, CT, 2004.
(25) Becke, A. D. *J. Chem. Phys.* **1993**, *98*, 5648–5652.
(26) Lee, C.; Yang, W.; Parr, R. G. *Phys. Rev. B: Condens. Matter Mater. Phys.* **1988**, *37*, 785–789.
(27) Hay, P. J.; Wadt, W. R. *J. Chem. Phys.* **1985**, *82*, 299–310.
(28) Höllwart, A.; Böhme, M.; Dapprich, S.; Ehlers, A. W.; Gobbi, A.; Jonas, V.; Köhler, K. F.; Stegmann, R.; Veldkamp, A.; Frenking, G. *Chem. Phys. Lett.* **1993**, *208*, 237–240.
(29) Hehre, W. J.; Ditchfield, R.; Pople, J. A. *J. Chem. Phys.* **1972**, *56*, 2257–2261.

performed on all optimized structures to characterize the stationary points as minima or transition states, as well as for the calculation of gas-phase zero-point energies (ZPE), enthalpies (*H*), entropies (*S*), and Gibbs energies (*G*) at 298.15 K. In addition, the stability of the wave function was checked[32,33] in the most critical regions of the potential energy surface (i.e., transition states). In all cases the wave functions were found to be stable with respect to relaxing spin and symmetry constraints. Solvent effects were taken into account by means of PCM[34,35] (methanol, $\epsilon = 32.63$) single-point calculations at the gas-phase optimized geometries. Finally, to check the basis set dependence on the results, an alternative extended basis set (BS2) was used to recalculate the potential energy profiles in methanol (PCM) by means of single-point calculations at the previously gas-phase optimized geometries: the all-electron basis DZVP[36,37] was used to represent the metal, the 6-31G(d,p) basis was used for all hydrogen atoms, and the rest of the atoms (C, N, O, and P) were represented by means of the 6-31G(d) basis.

Results and Discussion

Neutral Mechanism. As mentioned above, the metal complexes used in the parallel NMR experimental investigation were Pd(II) species of the type $Pd(P_2)(OTf)_2$. These species evolve under the reaction conditions to yield the active catalyst. In the following section we assume that the Pd(II) complex is reduced, in situ, to a Pd(0) species of the type $Pd(P_2)$ in the first step. This change has been accepted for many palladium- and platinum-catalyzed reactions.[38,39]

Throughout the following sections we first describe the mechanistic findings obtained using a bidentate phosphine ligand (dhpe = $PH_2CH_2CH_2PH_2$) in the gas phase and then highlight the differences that are introduced by changing to monodentate phosphines (PH_3) before considering the effect of solvent.

Pd(dhpe) ($\mathbf{1_{NB}}$)[40] is therefore the starting point from which a neutral catalytic hydrogenation cycle is constructed. The next step in the reaction must involve either H_2 addition or alkyne coordination. H_2 addition to $\mathbf{1_{NB}}$ was found to be exothermic by just 11.2 kJ·mol^{-1}, while the coordination of acetylene to form Pd(dhpe)(HC≡CH) ($\mathbf{2_{NB}}$) is exothermic by 107.9 kJ·mol^{-1}. Thus the most likely route for hydrogenation by a bisphosphine-based palladium(0) precursor would involve alkyne coordination to form $\mathbf{2_{NB}}$. When the addition of H_2 to $\mathbf{2_{NB}}$ was probed, however, no route to the formation of Pd(dhpe)(HC≡CH)$(H)_2$ could be located. This matches the deductions of previous workers[41] and is also consistent with the fact that pathways involving the direct addition of H_2 to the external face of the bound alkyne are unfavored. We therefore considered the energetics associated with the formation of Pd(κ^1P-dhpe)(HC≡CH) ($\mathbf{3_{NB}}$) from $\mathbf{2_{NB}}$ via dissociation of one phosphine arm. Dissociation of one arm of the dhpe ligand of $\mathbf{2_{NB}}$ results in $\mathbf{3_{NB}}$ being 39.5 kJ·mol^{-1} higher in energy than $\mathbf{2_{NB}}$. Subsequent calculations revealed that the binding of H_2 to Pd(κ^1P-dhpe)(HC≡CH) ($\mathbf{3_{NB}}$), which forms Pd(κ^1P-dhpe)(HC≡CH)$(H)_2$ ($\mathbf{4_{NB}}$), is exothermic by 10.6 kJ·mol^{-1}; the overall energy change on going from $\mathbf{1_{NB}}$ plus H_2 and HC≡CH to $\mathbf{4_{NB}}$ is exothermic by 79.0 kJ·mol^{-1}. The conversion of $\mathbf{3_{NB}}$ to $\mathbf{4_{NB}}$ therefore involves the pairwise coordination of a dihydrogen molecule and is consistent with the experimental data illustrated in the right side of Figure 1 that require a PHIP-active reaction pathway.

Scheme 1. DFT-Derived Scheme for Hydrogenation by a Neutral Palladium(0) Bisphosphine Complex[a]

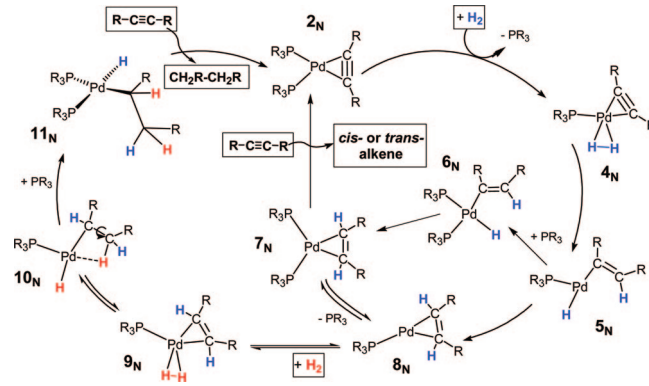

[a] In the calculations the alkyne is acetylene and the phosphine either dhpe or PH_3.

Hydride transfer in $\mathbf{4_{NB}}$ then proceeds to form Pd(κ^1P-dhpe)(CH=CH_2)(H) ($\mathbf{5_{NB}}$). The transformation from $\mathbf{4_{NB}}$ to $\mathbf{5_{NB}}$ proved to involve a relatively high energy transition state, ($\mathbf{4_{NB}}$→$\mathbf{5_{NB}}$)**TS**, of 83.7 kJ·mol^{-1}, which is close to the upper limit for reactions taking place at room temperature. Since species $\mathbf{5_{NB}}$ is 14-electron, it will readily recoordinate the phosphine to form Pd(dhpe)(CH=CH_2)(H) ($\mathbf{6_{NB}}$). This exothermic phosphine coordination step yields an energy return of 114.0 kJ·mol^{-1}. The transfer of the metal hydride of $\mathbf{6_{NB}}$ to the vinyl ligand was found to take place via a low-energy transition state, ($\mathbf{6_{NB}}$→$\mathbf{7_{NB}}$)**TS**, of only 7.3 kJ·mol^{-1} and leads to the formation of the corresponding 16-electron alkene complex Pd(dhpe)(η^2-CH_2=CH_2) ($\mathbf{7_{NB}}$). The process of alkyne semihydrogenation is then completed by alkene liberation from $\mathbf{7_{NB}}$ and the binding of acetylene to regenerate $\mathbf{2_{NB}}$. The replacement of C_2H_4 by CH≡CH proved to be favored by 7.5 kJ·mol^{-1}, confirming that this process is viable from a thermodynamic perspective.

This sequence of reaction steps accounts for the formation of *cis*-alkene products since hydride ligand transfer takes place on the internal face of the metal-vinyl (step $\mathbf{6_{NB}}$ to $\mathbf{7_{NB}}$). Scheme 1 summarizes the transformations that are involved in achieving this result, while the corresponding energy profiles are shown in Figure 2. These results are not surprising since complexes of the type Pd(LL)(alkene) are well-known[42–44] and have been

(30) Hariharan, P. C.; Pople, J. A. *Theor. Chim. Acta.* **1973**, *28*, 213–222.
(31) Francl, M. M.; Pietro, W. J.; Hehre, W. J.; Binkley, J. S.; Gordon, M. S.; DeFrees, D. J.; Pople, J. A. *J. Chem. Phys.* **1982**, *77*, 3654–3655.
(32) Seeger, R.; Pople, J. A. *J. Chem. Phys.* **1977**, *66*, 3045–3050.
(33) Bauernschmitt, R.; Ahlrichs, R. *J. Chem. Phys.* **1996**, *104*, 9047–9052.
(34) Tomasi, J.; Persico, M. *Chem. Rev.* **1994**, *94*, 2027–2094.
(35) Amovilli, C.; Barone, V.; Cammi, R.; Cancès, E.; Cossi, M.; Mennucci, B.; Pomelli, C. S.; Tomasi, J. *J. Adv. Quantum Chem.* **1999**, *32*, 227–261.
(36) Godbout, N.; Salahub, D. R.; Andzelm, J.; Wimmer, E. *Can. J. Chem.* **1992**, *70*, 560–571.
(37) Sosa, C.; Andzelm, J.; Elkin, B. C.; Wimmer, E.; Dobbs, K. D.; Dixon, D. A. *J. Phys. Chem.* **1992**, *96*, 6630–6636.
(38) Amatore, C.; Jutand, A. *Acc. Chem. Res.* **2000**, *33*, 314–321.
(39) Espinet, P.; Echavarren, A. M. *Angew. Chem., Int. Ed.* **2004**, *43*, 4704–4734.
(40) In the rest of this section the subscript N will be used to denote neutral intermediates. A second subscript M or B indicates monodentate phosphine-based species (PH_3) or bidentate phosphine-based species (dhpe), respectively.
(41) Dedieu, A.; Humbel, S.; Elsevier, C.; Grauffel, C. *Theor. Chem. Acc.* **2004**, *112*, 305–312.
(42) Pan, Y.; Mague, J. T.; Fink, M. J. *Organometallics* **1992**, *11*, 3495–3497.
(43) Ozawa, F.; Sugawara, M.; Hayashi, T. *Organometallics* **1994**, *13*, 3237–3243.
(44) Moncarz, J. R.; Brunker, T. J.; Jewett, J. C.; Orchowski, M.; Glueck, D. S. *Organometallics* **2003**, *22*, 3205–3221.

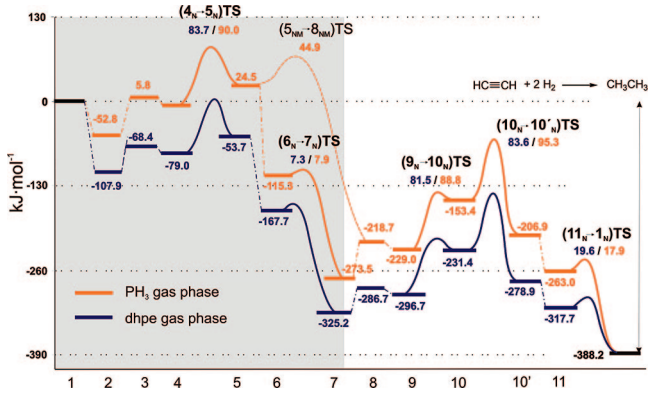

Figure 2. DFT-based potential energy profiles for the neutral alkyne hydrogenation cycle. The blue lines denote the dhpe-based mechanism, while the orange ones are for the PH_3-based system. The shadowed area indicates the sequence of steps necessary for *cis*-alkene formation. The presented energies are relative to $Pd(0)P_2$, HC≡CH, and $2H_2$, while the values for the transition states are relative to the preceding local minimum.

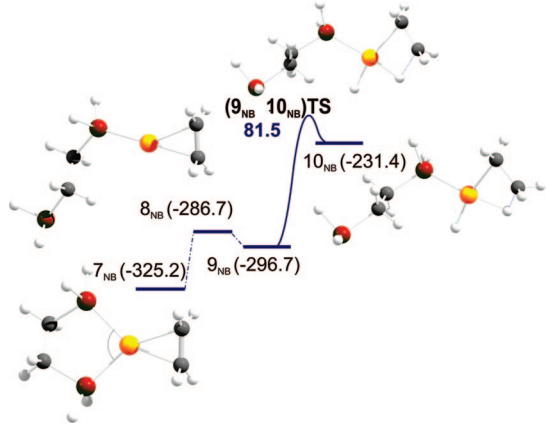

Figure 3. Potential energy profile for the conversion of $\mathbf{7_{NB}}$ to $\mathbf{10_{NB}}$. The quoted energies (kJ·mol^{-1}) are relative to $Pd(0)P_2$, HC≡CH, and $2H_2$, while the value for the transition state is relative to $\mathbf{9_{NB}}$.

used as catalyst precursors for this reaction.[7,45] In one such example,[7] Elsevier and co-workers detected PHIP-enhanced NMR signals for the reaction products of the semihydrogenation of alkynes catalyzed by Pd(0) species bearing α-diimine ligands, although no reaction intermediates were detected. This observation would therefore be satisfied by such a reaction mechanism.

***cis/trans* Alkene Isomerization.** One major experimental observation that is associated with reactions involving alkyne hydrogenation is *cis/trans* alkene isomerizarization.[5,6,45] In order for this process to happen, the alkene substrate must be bound to the metal. Species $\mathbf{7_{NB}}$ corresponds to a potential starting point for this process, but calculations reveal that H_2 addition to it is unfavorable. In this case, the most feasible reaction pathway involves again phosphine dissociation to form Pd(κ^1P-dhpe)(η^2-CH_2=CH_2) ($\mathbf{8_{NB}}$), a process that is endothermic by only 38.5 kJ·mol^{-1}. Coordination of a second molecule of dihydrogen to $\mathbf{8_{NB}}$ is slightly exothermic, yielding Pd(κ^1P-dhpe)(η^2-CH_2=CH_2)$(H)_2$ ($\mathbf{9_{NB}}$), which forms the alkyl hydride Pd(κ^1P-dhpe)(CH_2CH_3)(H) ($\mathbf{10_{NB}}$) after hydride migration.

(45) van Laren, M. W.; Elsevier, C. J. *Angew. Chem., Int. Ed.* **1999**, *38*, 3715–3717.

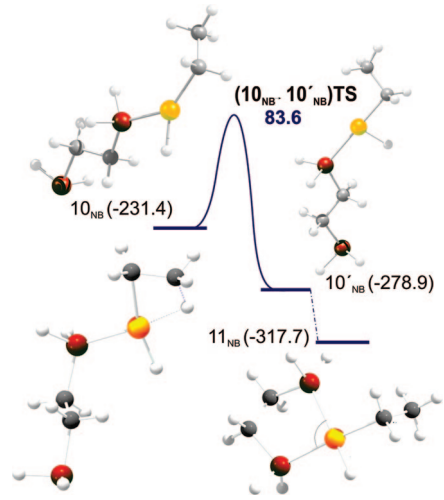

Figure 4. Potential energy profile for the transformation of $\mathbf{10_{NB}}$ to $\mathbf{11_{NB}}$. The energies are relative to $Pd(0)P_2$, HC≡CH, and $2H_2$, while the value for the transition state is with respect to $\mathbf{10_{NB}}$.

These DFT data reveal that 14-electron $\mathbf{10_{NB}}$ is stabilized by an agostic interaction as illustrated in Figure 3 (Pd···H = 1.875 Å, H−C = 1.192 Å). The role of analogous agostic-stabilized intermediates in β-hydride elimination reactions was considered by Morokuma in an earlier ab initio study of this system.[46]

The energy barrier for the hydride transfer step, ($\mathbf{9_{NB}}$→$\mathbf{10_{NB}}$)**TS**, proved to be 81.5 kJ·mol^{-1}, but phosphine dissociation from $\mathbf{7_{NB}}$ makes the overall barrier to this route a potentially prohibitive 109.9 kJ·mol^{-1}. While the recoordination of phosphine to $\mathbf{10_{NB}}$ to yield the alkyl hydride Pd(dhpe)(CH_2CH_3)(H) ($\mathbf{11_{NB}}$) provides an energy return of 109.6 kJ·mol^{-1}, the barriers associated with its formation mean its production must be questionable; in this respect, internal reorganization in $\mathbf{10_{NB}}$ (barrier of 83.6 kJ·mol^{-1} (($\mathbf{10_{NB}}$→$\mathbf{10'_{NB}}$)**TS**)) is necessary prior to phosphine coordination, which is barrierless (Figure 4).

In order for alkene isomerization to take place, an equilibrium must exist between the alkyl-palladium complex $\mathbf{11_{NB}}$ and the palladium η^2-alkene complex $\mathbf{7_{NB}}$, but according to these DFT data such an equilibration must be slow. The individual steps in this process involve β-H transfer and rotation about the C−C bond of the alkyl ligand in $\mathbf{10_{NB}}$ or $\mathbf{11_{NB}}$. While the barrier for C−C rotation in $\mathbf{10_{NB}}$ proved to be 20.0 kJ·mol^{-1}, a lower barrier is expected in $\mathbf{11_{NB}}$, which is not agostic stabilized. This sequence of steps is illustrated in Figures 3 and 4, and in Scheme 1, but the energy costs in following them are likely to be prohibitive in our systems. Nonetheless related isomerization mechanisms have been considered to operate by Bargon and more recently by Elsevier.[7,47]

Over-reduction to the Alkane. Calculations showed that alkane elimination from $\mathbf{11_{NB}}$ is very exothermic, releasing 70.5 kJ·mol^{-1}. The barrier to this transformation, ($\mathbf{11_{NB}}$→$\mathbf{1_{NB}}$)**TS**, is only 19.6 kJ·mol^{-1}, and hence the reaction should be facile. In contrast, the overall barrier to transform $\mathbf{11_{NB}}$ back into the alkene precursor $\mathbf{7_{NB}}$ is 169.9 kJ·mol^{-1} (Figures 3 and 4). Reductive elimination of the alkane from $\mathbf{11_{NB}}$ is therefore expected to predominate if this species if formed. Since the experimental data indicate little alkane formation, however, the formation of $\mathbf{11_{NB}}$ is inconsistent with the experimental results.

(46) Koga, N.; Obara, S.; Kitaura, K.; Morokuma, K. *J. Am. Chem. Soc.* **1985**, *107* (24), 7109–7116.

(47) Harthun, A.; Giernoth, R.; Elsevier, C. J.; Bargon, J. *J. Chem. Commun.* **1996**, *21*, 2483–2484.

Table 1. Relative Energies (ΔE, kJ mol^{-1}) for the Species Involved in the Neutral Mechanism

	PH_3 (NM designation)		dhpe (NB designation)	
structure	gas phase	methanol	gas phase	methanol
$\mathbf{1_N}$ + acetylene + $\mathbf{2H_2}$	0	0	0	0
$\mathbf{2_N}$ + $2H_2$	−52.8	−49.2	−107.9	−99.2
$\mathbf{3_N}$ + $2H_2$ (+PH_3)	5.8	25.2	−68.4	−54.2
$\mathbf{4_N}$ + H_2 (+PH_3)	−6.3	1.1	−79.0	−63.7
$\mathbf{(4_N \rightarrow 5_N)TS}$ + H_2 (+PH_3)	83.7	78.5	4.7	6.1
$\mathbf{5_N}$ + H_2 (+PH_3)	24.5	−4.9	−53.7	−74.2
$\mathbf{6_{N(cis)}}$ + H_2	−115.3	−123.3	−167.7	−177.3
$\mathbf{(6_N \rightarrow 7_N)TS}$ + H_2	−107.4	−106.5	−160.2	−159.3
$\mathbf{7_N}$ + H_2	−273.5	−265.2	−325.2	−309.9
$\mathbf{(5_{NM} \rightarrow 8_{NM})TS}$ + H_2 (+PH_3)	69.4	66.0	−	−
$\mathbf{8_N}$ + H_2 (+PH_3)	−218.7	−207.0	−286.7	−267.5
$\mathbf{9_N}$ (+PH_3)	−229.0	−218.0	−296.7	−276.4
$\mathbf{(9_N \rightarrow 10_N)TS}$ (+PH_3)	−140.2	−148.5	−215.3	−212.6
$\mathbf{10_N}$ (+PH_3)	−153.4	−163.9	−231.4	−231.6
$\mathbf{(10_N \rightarrow 10'_N)TS}$ (+PH_3)	−58.1	−73.0	−147.8	−135.5
$\mathbf{10'_N}$ (+PH_3)	−206.9	−202.9	−317.7	−286.3
$\mathbf{11_N}$	−263.0	−273.1	−317.7	−326.6
$\mathbf{(11_N \rightarrow 1_N)TS}$	−245.1	−245.5	−298.1	−292.5
$\mathbf{1_N}$ + ethane	−388.2	−387.6	−388.2	−387.6

Phosphine Effects. The computational results reported here with the dhpe ligand can be related to the experimental results obtained with bidentate chelating phosphines such as bcope and ^{t}bucope. We have extended the theoretical study also considering the ligand PH_3, a closer model to the monodentate phosphine PEt_3 studied experimentally. We have followed the analogous reaction sequence as already described for dhpe. Now, the loss of PH_3 is slightly more endothermic than that seen for an arm of the dhpe ligand (Figure 2). Furthermore, the release in energy resulting from alkyne binding in $\mathbf{1_{NM}}$ to yield $\mathbf{2_{NM}}$ is only 52.8 kJ·mol^{-1} as opposed to 107.9 kJ·mol^{-1}in $\mathbf{1_{NB}}$.

Other differences include phosphine coordination to $Pd(PH_3)(CH{=}CH_2)(H)$, $\mathbf{5_{NM}}$, which in this case leads to both *cis* and *trans* isomers of $Pd(PH_3)_2(CH{=}CH_2)(H)$ ($\mathbf{6_{NMcis}}$, $\mathbf{6_{NMtrans}}$), where the *cis* isomer is favored by 20.6 kJ·mol^{-1}. The transfer of the metal hydride of $\mathbf{6_{NMcis}}$ to the vinyl ligand was found to take place via a transition state, $\mathbf{(6_{NM} \rightarrow 7_{NM})TS}$, that provides an energy barrier of only 7.9 kJ·mol^{-1}; this is similar to the analogous dhpe barrier of 7.3 kJ·mol^{-1}. This step yields the 16-electron alkene complex $Pd(PH_3)_2(\eta^2\text{-}CH_2{=}CH_2)$ ($\mathbf{7_{NM}}$). An alternative route featuring C−H bond formation via the monophosphine derivative $Pd(PH_3)(CH{=}CH_2)(H)$ ($\mathbf{5_{NM}}$) proved to have a much higher barrier, $\mathbf{(5_{NM} \rightarrow 8_{NM})TS}$, of 44.9 kJ·mol^{-1}. This route yields the unsaturated species $Pd(PH_3)(\eta^2\text{-}CH_2{=}CH_2)$ ($\mathbf{8_{NM}}$) and does not compete with that via $\mathbf{6_{NM}}$.

Despite these differences, the energy barriers for the two neutral mechanisms do not change sufficiently to suggest that replacing a bidentate phosphine with a monodentate one leads to a substantial variation in the viability of alkyne hydrogenation via Pd(0) species.

Solvent Effects. The introduction of a continuum-based solvent model for methanol does not result in any large-scale changes in the associated energy profiles for the neutral reaction cycle (see Supporting Information). The energy barriers for the transition states $\mathbf{(4_N \rightarrow 5_N)TS}$ and $\mathbf{(9_N \rightarrow 10_N)TS}$ are however lowered by ca. 14 and ca. 19 kJ·mol^{-1}, respectively. The energies of all the associated intermediates with both dhpe and PH_3 in the gas phase and methanol are listed in Table 1. The corresponding structures of all the species can be found in the Supporting Information. Additional Gibbs energy data that are consistent with the deductions based on the potential energy data are also listed here.

Cationic Mechanism. We now consider an alternative mechanism based on a cationic palladium monohydride complex of the type $[Pd(P_2)(H)]^+$. The generation of such monohydride complexes from palladium(II) triflates and methanol has been seen experimentally.[3,15] Indeed, in our experimental investigation,[15] [Pd(^{t}bucope)$(OTf)_2$] was found to react slowly in methanol-d_4 in the presence of pyridine to form [Pd(^{t}bucope)(D)(py)]$^+$. This complex then reacted instantaneously with diphenylacetylene to give [Pd(^{t}bucope)(PhC≡C(D)Ph)(py)]$^+$, and with *cis*-stilbene to form [Pd(^{t}bucope)(PhCHCHDPh)]$^+$. The activity of such species in the semihydrogenation reaction has therefore been established.

The structure of the model complex $[Pd(dhpe)(H)]^+$ ($\mathbf{1_{CB}}$)[48] is T shaped (P−Pd−P angle of 88.6°) with the hydride ligand lying *trans* to one of the phosphorus centers. The Pd−P bond for the ligand that is *trans* to hydride is subject to elongation in $\mathbf{1_{CB}}$, where it is 2.489 Å compared to 2.234 Å for the remaining Pd−P bond.

***cis*-Alkene Formation.** Like in the neutral mechanism, coordination of the alkyne to the precursor, $\mathbf{1_{CB}}$, is exothermic, in this case by 122.3 kJ·mol^{-1}, and yields the complex $[Pd(dhpe)(HC{\equiv}CH)(H)]^+$ ($\mathbf{2_{CB}}$). Hydride migration to the alkyne ligand of $\mathbf{2_{CB}}$ produces the vinyl complex $[Pd(dhpe)(CH{=}CH_2)]^+$ ($\mathbf{3_{CB}}$). Calculations reveal that the associated energy barrier to reach the transition state $\mathbf{(2_{CB} \rightarrow 3_{CB})TS}$ for this process is only 5.2 kJ·mol^{-1} (see Scheme 2 and Figure 5). In order for the reaction to proceed further, H_2 addition to $\mathbf{3_{CB}}$ is necessary, which forms $[Pd(dhpe)(H)_2(CH{=}CH_2)]^+$ ($\mathbf{4_{CB}}$). This step proved to be slightly exothermic with an energy return of just 27.0 kJ·mol^{-1}.

$\mathbf{4_{CB}}$ exhibits a number of remarkable structural features. First, there is little lengthening of the H−H distance upon coordination to the metal center, which is 0.77 Å versus the 0.74 Å found for free H_2. Second, the Pd−H distances are particularly long at 1.968 Å (average), where a more usual distance would be ca. 1.6 Å. In addition, the energy change associated with H_2 binding to form $\mathbf{4_{CB}}$ is only 27.0 kJ·mol^{-1} and therefore consistent with a weak bonding interaction in this dihydrogen rather than dihydride complex.[49–51] This situation is also reflected in related species that were described earlier in the neutral section (see Supporting Information).

Hydride migration to give the alkene hydride $[Pd(dhpe)(H)(\eta^2\text{-}CH_2{=}CH_2)]^+$ ($\mathbf{5_{CB}}$) is very exothermic at 129.3 kJ·mol^{-1}, and the energy barrier $\mathbf{(4_{CB} \rightarrow 5_{CB})TS}$ is only 38.4 kJ·mol^{-1}. Consequently, the large barrier to the reverse process suggests that transfer of the metal hydride to the vinyl ligand in $\mathbf{4_{CB}}$ is irreversible. The combination of these changes also means that, for the dhpe system, moving from $[Pd(dhpe)(H)]^+$ ($\mathbf{1_{CB}}$), H_2, and HC≡CH to $[Pd(dhpe)(H)(\eta^2\text{-}CH_2{=}CH_2)]^+$ ($\mathbf{5_{CB}}$) is exothermic by 358.5 kJ·mol^{-1}. At this point, if the *cis*-alkene is to be liberated, acetylene substitution is necessary. Calcula-

(48) Following the same numbering system as in the previous sections, throughout the rest of this section the subscript C will be used to denote cationic intermediates. A second subscript M or B indicates monodentate phosphine-based species (PH_3) or bidentate phosphine-based species (dhpe), respectively.

(49) Maseras, F.; Lledós, A.; Clot, E.; Eisenstein, O. *Chem. Rev.* **2000**, *100*, 601–636.

(50) Heinekey, D. M.; Lledós, A.; Lluch, J.-M. *Chem. Soc. Rev.* **2004**, *33*, 175–182.

(51) Kubas, G. J.; Ryan, R. R.; Swanson, B. I.; Vergamini, P. J.; Wasserman, H. J. *J. Am. Chem. Soc.* **1984**, *106*, 451–452.

(52) Deibele, C.; Permin, A. B.; Petrosyan, V. S.; Bargon, J. *Eur. J. Inorg. Chem.* **1998**, *1915*, 1923.

Scheme 2. DFT-Derived Scheme for Hydrogenation by a Palladium Monohydride Bisphosphine cation. In the calculations the alkyne is acetylene and the phosphine either dhpe or PH_3

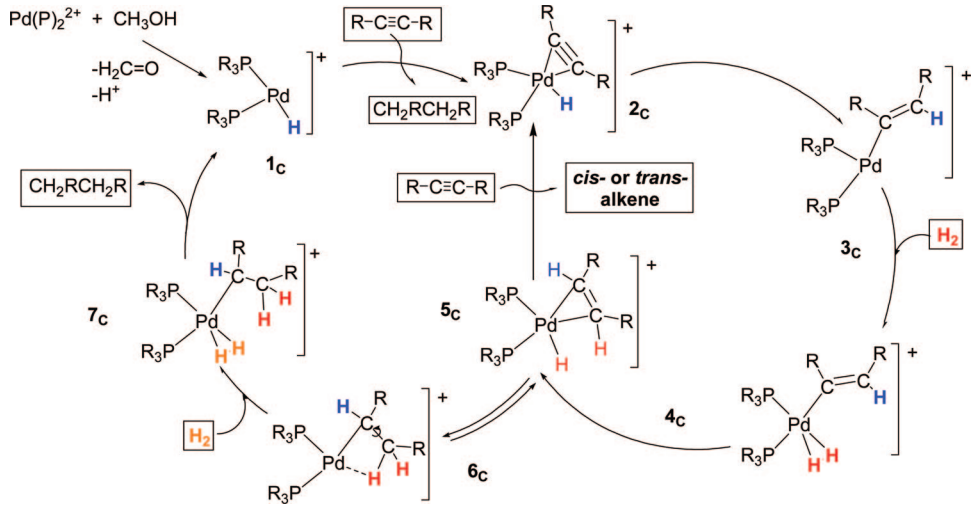

tions indicate that this process is slightly endothermic for the dhpe system by 11.3 kJ·mol^{-1}.

***cis/trans* Alkene Isomerization and Rationalization of the Experimental Observation of the PHIP Effect.** It should be noted that the alkene molecules formed by this route would not give rise to the PHIP-enhanced resonances that are seen experimetally, since the reaction does not involve the pairwise transfer of a *para*-hydrogen molecule into the product.[52] Hydrogen scrambling is therefore necessary if two hydrogen atoms from a single *para*-hydrogen molecule are to be placed within the same alkene. In view of the fact that since *cis/trans* alkene isomerization is seen experimentally, the calculations should be consistent with these observations:

The starting point for *cis/trans* isomerization would be hydride migration from the η^2-alkene hydride [Pd(dhpe)(H)(η^2-CH_2=CH_2)]$^+$ (**5$_{CB}$**), where the alkene, the metal center, and the hydride are almost coplanar. This yields [Pd(dhpe)(CH_2CH_3)]$^+$ (**6$_{CB}$**) in a process that takes place with a very low energy barrier, as illustrated in Figure 6 [(**5$_{CB}$**→**6$_{CB}$**)**TS**, ΔE = 3.7 kJ·mol^{-1}].

Our calculations show that **6$_{CB}$** actually corresponds to an agostic-alkyl complex. Now, C−C bond rotation and β-H elimination in **6$_{CB}$** to form **5$_{CB}$** would account for *cis/trans* alkene isomerization. The formation of **5$_{CB}$** from **6$_{CB}$** is indeed predicted since the barrier for the reverse process is only 37.9 kJ·mol^{-1}, and C−C bond rotation in **6$_{CB}$** is facile with an energy barrier of ca. 16 kJ·mol^{-1}. Furthermore, the barrier to alkene rotation in **5$_{CB}$** is 17.8 kJ·mol^{-1} and comparable to that for C−C bond rotation in **6$_{CB}$**. The latter process, in conjunction with the alkene-hydride/alkyl isomerization can place two hydrogen atoms from the same molecule of hydrogen into the alkene. This process therefore provides a reaction sequence that matches with the experimental observation of PHIP-enhanced resonances in both the *cis*- and *trans*-alkenes formed in the hydrogenation reaction. These processes are depicted in Scheme 3.

The product of hydride transfer, [Pd(dhpe)(CH_2CH_3)]$^+$ (**6$_{CB}$**), should be regarded as a model of the alkyl palladium complexes detected in the PHIP NMR studies of this reaction. Experimentally, the NMR resonances for the analogous species proved to have very similar chemical shifts regardless of the solvent or, indeed, whether pyridine was added to the solution. This indicates that there is no solvent or pyridine coordination in the experimentally detected alkylpalladium intermediates [Pd(bcope)(CHPhCH$_2$Ph)](OTf) and [Pd(^{t}bucope)(CHPhCH$_2$

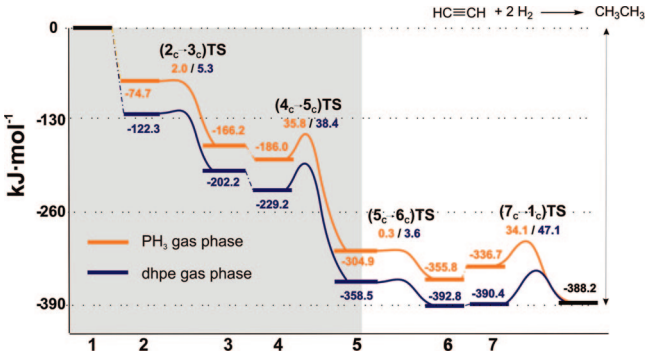

Figure 5. DFT-derived potential energy profiles for the cation-based semihydrogenation cycle for dhpe (blue lines) and PH_3 (orange lines) in the gas phase. The shadowed area accounts for *cis*-alkene formation. Energies are relative to $PdP_2(H)^+$, HC≡CH, and $2H_2$, while the values for the transition states are with respect to the immediately preceding local minimum.

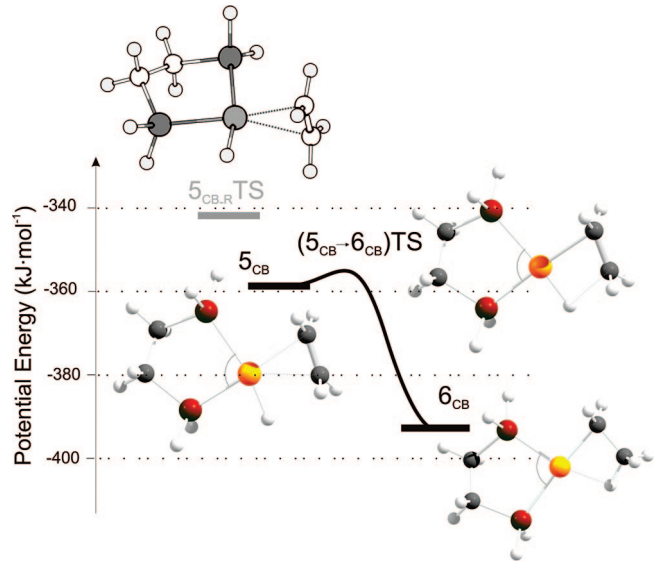

Figure 6. Potential energies and optimized structures for **5$_{CB}$**, **6$_{CB}$**, and the transition states for hydride transfer (**5$_{CB}$**→**6$_{CB}$**) and alkene rotation (**5$_{CB_R}$TS**). Energies are relative to PdP_2H^+, HC≡CH, and $2H_2$.

Scheme 3. Mechanism for *cis/trans* Alkene Isomerization and Hydrogen Scrambling[a]

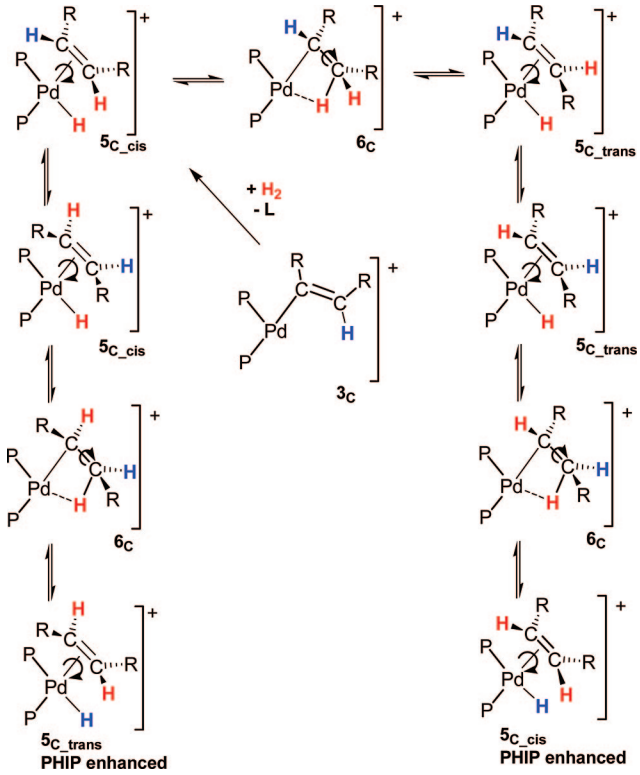

[a] The red hydrogen atoms represent atoms from the same *para*-hydrogen molecule, which can be placed onto the same alkene ligand by hydrogen atom scrambling. In the calculations, PP is dhpe and R is H.

Ph)](OTf). Experimentally, secondary coordination via the phenyl ring was, however, shown to account for the stability of these complexes rather than an agostic C−H bond interaction. We will come back to this point later.

The presence of an β-agostic interaction in $\mathbf{6_{CB}}$ is consistent with related experimental observations made by Heaton and Iggo et al. on $[Pd(P)_2(CH_2CH_3)]^+$ [where PP = 1,2-$(CH_2PBu^t_2)_2C_6H_4$][4] where an agostic interaction is indicated in solution. They observed coalescence of the C_α and C_β carbon resonances of the ethyl ligand upon heating, thereby confirming the reversibility of the hydride transfer step. Such a β-hydride elimination/alkene insertion process also features in palladium(II) and nickel(II) alkene polymerization.[53–55] A further experimental observation that supports these deductions was made after the addition of *cis*-stilbene to the monodeuteride complex [Pd(^{t}bucope)(D)(py)]$^+$. Under the reaction conditions, the alkyl palladium complex [Pd(^{t}bucope)(PhCHCDHPh)]$^+$, PhHC═CDPh, and the monohydride [Pd(^{t}bucope)(H)(py)]$^+$ were detected by NMR spectroscopy after a few seconds.

Over-reduction to Alkane. If an alkane product is to be formed in this reaction, $[Pd(dhpe)(CH_2CH_3)]^+$ ($\mathbf{6_{CB}}$) must coordinate a second molecule of dihydrogen to yield [Pd(dhpe)$(CH_2CH_3)(H)_2]^+$ ($\mathbf{7_{CB}}$). Reductive C−H coupling in $\mathbf{7_{CB}}$ must then follow. A minimum has been located in the reaction's potential energy surface for $\mathbf{7_{CB}}$ with the addition of H_2 to $\mathbf{6_{CB}}$ being endothermic by only 2.4 kJ·mol^{-1}. The breaking of the β-agostic H−Pd interaction in $\mathbf{6_{CB}}$ provides the main barrier to this transformation. An estimate of the energy cost for this process has been obtained by monitoring the rotation of the alkyl ligand about the Pd−Cα bond since when it attains an orientation that is 60° out of the coordination plane of the palladium, the C−H bond distance is 3.08 Å and a Pd−H bonding interaction is no longer supported. This point is achieved with an energy cost of ca. 25 kJ·mol^{-1}, although the barrier to complete 360° rotation of the alkyl ligand is 35 kJ·mol^{-1}. In addition, the energy barrier for the elimination of ethane in $\mathbf{7_{CB}}$, $(\mathbf{7_{CB}}\rightarrow\mathbf{1_{CB}})\mathbf{TS}$, was found to be 47.1 kJ·mol^{-1}, with the overall barrier for alkane elimination from $\mathbf{6_{CB}}$ being 49.5 kJ·mol^{-1}. In contrast, it has been previously noted that reverse β-hydrogen elimination from $\mathbf{6_{CB}}$ has a lower barrier at 37.9 kJ·mol^{-1}. Consequently, as Figure 5 confirms, alkene isomerization is preferred over alkane formation, in agreement with the previously reported experimental observations.

Role of the Substrate. An extensive study of the effect that the alkyne has on the mechanism of semihydrogenation is beyond the scope of this DFT investigation. However, we are concerned about the exact nature of the alkylpalladium complexes detected experimentally. The calculations confirm that $\mathbf{7_C}$ is stabilized by a β-agostic interaction, yet this situation is not reflected in the PHIP NMR study of [Pd(bcope)$(CHPhCH_2Ph)]$(OTf), where normal carbon−hydrogen coupling constant values were determined.[15] Phenyl rings were therefore introduced into the alkyl ligand employed in the DFT study in order to mimic more closely the experimental situation. When $[Pd(dhpe)(CHPhCH_2Ph)]^+$ was considered in this way, two isomers bearing β-agostic interactions were identified. One of these isomers ($\mathbf{6_{CB\_Ph\text{-}cis}}$) is the result of hydride migration in [Pd(dhpe)(H)(η^2-*cis*-CHPh═CHPh)]$^+$, while the second ($\mathbf{6_{CB\_Ph\text{-}trans}}$) relates to [Pd(dhpe)(H)(η^2-*trans*-CHPh═CHPh)]$^+$, the latter being more stable by 11.5 kJ·mol^{-1} (Figure 7). A third isomer was however found ($\mathbf{6_{CB\_Ph\text{-}benzyl}}$), which was stabilized by 49.4 kJ·mol^{-1} relative to $\mathbf{6_{CB\_Ph\text{-}cis}}$. This isomer features an interaction between the metal and the phenyl ring bonded to the α-carbon of the alkyl ligand. Such a species can be described as an η^3-benzyl complex[56] and has been shown to participate in β-alkyl migratory insertion in Heck-type reactions with vinyl arenes.[57,58] This situation matched that found experimentally[15] and suggests an even greater preference for alkene isomerization versus alkane formation when diphenylacetylene is used as the reaction substrate since interaction of the metal center with H_2 will be even more difficult. This information indicates that the substrate plays an important role in stabilizing the alkylpalladium intermediates detected during the PHIP NMR studies.

Phosphine Effect. When an analogous analysis was completed on the PH_3 derivative, no qualitative differences were found to exist in the associated reaction's energy profile. Energy profiles for the cationic cycle with dhpe and PH_3 as the model phosphine in the gas phase and tabulated data can be found in the Supporting Information. We (supplementary) and others have considered phosphine loss pathways in such a cationic cycle.[59]

(53) Werner, H.; Feser, R. *Angew. Chem., Int. Ed. Engl.* **1979**, *18* (22), 157–158.
(54) Shultz, L. H.; Tempel, D. J.; Brookhart, M. *J. Am. Chem. Soc.* **2001**, *123*, 11539–11555.
(55) Leatherman, M. D.; Svedja, S. A.; Johnson, L. K.; Brookhart, M. *J. Am. Chem. Soc.* **2003**, *125*, 308–3081.
(56) del Río, I.; Claver, C.; van Leeuwen, P. W. N. M. *Eur. J. Inorg. Chem.* **2001**, *2719*, 2738.
(57) Rix, F. C.; Brookhart, M.; White, P. S. *J. Am. Chem. Soc.* **1996**, *118*, 2436–2448.
(58) Hii, K. K. M.; Claridge, T. D. W.; Giernoth, R.; Brown, J. M. *Adv. Synth. Catal.* **2004**, *346*, 983–988.
(59) Ahlquist, M.; Fristrup, P.; Tanner, D.; Norrby, P. O. *Organometallics* **2006**, *25* (8), 2066–2073.

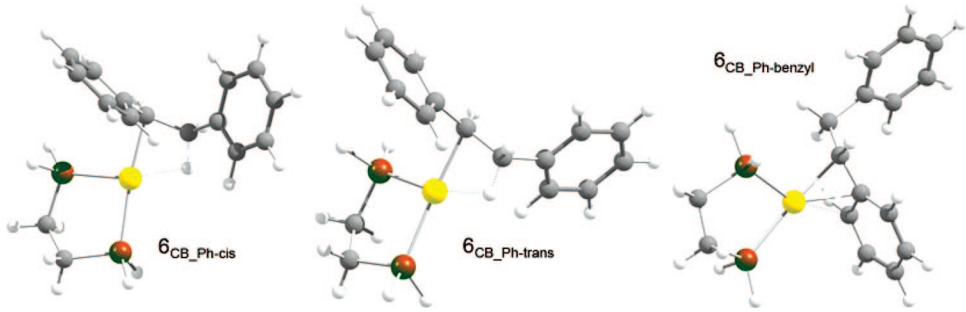

Figure 7. Optimized structures for three isomers of $[Pd(dhpe)(CHPh\text{-}CH_2Ph)]^+$. Both $\mathbf{6_{CB\_Ph\text{-}cis}}$ and $\mathbf{6_{CB\_Ph\text{-}trans}}$ feature a β-agostic interaction, while in $\mathbf{6_{CB\_Ph\text{-}benzyl}}$ there is an interaction between the palladium center and the phenyl ring on the α-carbon of the alkyl ligand.

Table 2. Relative Energies (ΔE, kJ·mol^{-1}) for the Species Involved in the Cationic Mechanism

	PH_3 (CM designation)		dhpe (CB designation)	
structure	gas phase	methanol	gas phase	methanol
$\mathbf{1_C}$ + acetylene + $2H_2$	0	0	0	0
$\mathbf{1_C\_S}$ + acetylene + $2H_2$ − MeOH	−96.4	−67.8	−136.6	−57.9
$\mathbf{1_C\_py}$ + acetylene + $2H_2$ − py	−127.4	−96.9	−163.5	−83.1
$\mathbf{2_C}$ + $2H_2$	−74.7	−53.8	−122.3	−70.5
$(\mathbf{2_C \rightarrow 3_C})\mathbf{TS}$ + $2H_2$	−72.7	−50.9	−117.1	−50.7
$\mathbf{3_C}$ + $2H_2$	−166.2	−148.8	−202.2	−162.2
$\mathbf{3_C\_S}$ + $2H_2$ − MeOH	−278.9	−235.9	−319.7	−216.4
$\mathbf{3_C\_py}$ + $2H_2$ − py	−300.0	−256.6	−334.8	−239.5
$\mathbf{4_C}$ + H_2	−186.0	−167.7	−229.2	−163.3
$(\mathbf{4_C \rightarrow 5_C})\mathbf{TS}$ + H_2	−150.2	−154.3	−190.7	−118.0
$\mathbf{5_C}$ + H_2	−304.9	−270.5	−358.5	−288.1
$(\mathbf{5_C \rightarrow 6_C})\mathbf{TS}$ + H_2	−314.3	−292.0	−354.8	−281.5
$\mathbf{6_C}$ + H_2	−355.8	−334.0	−392.8	−321.3
$\mathbf{6_C\_S}$ + H_2	−432.8	−397.0	−473.7	−380.4
$\mathbf{6_C\_py}$ + H_2 − py	−457.0	−420.0	−492.2	−401.4
$\mathbf{7_C}$	−336.7	−320.5	−390.4	−321.0
$(\mathbf{7_C \rightarrow 1_C})\mathbf{TS}$ + ethene	−302.5	−285.8	−343.3	−274.6
$\mathbf{1_C}$ + ethene	−388.2	−387.6	−388.2	−387.6

Not surprisingly, phosphine loss from these cationic species proves to be much harder than in the previously described neutral cycle. For example, phosphine dissociation from $\mathbf{3_{CM}}$ to yield $[Pd(PH_3)(CH{=}CH_2)]^+$ ($\mathbf{3_{CM}'}$) is hopelessly endothermic by 193.4 kJ·mol^{-1}. Nonetheless, evidence for phosphine dissociation has been found in our experimental investigations, where for example the tris-phosphine species [Pd(bcope)(κ^1-bcope)(H)]$^+$ has been detected.[15]

Solvent Effects. Methanol and Pyridine Coordination. The effect of methanol, as a solvent, has been taken into account by introducing a polarizable continuum solvent model (PCM). This process yielded results that were similar to those already discussed for the neutral mechanism. Thus, while changes in the values of the relative energies do take place, there are no substantive changes in the energy profiles. Interestingly, some of the energy barriers are actually higher when the continuum solvent model is applied, the most remarkable corresponding to the change $(\mathbf{2_{CB} \rightarrow 3_{CB}})\mathbf{TS}$, which is 5.3 kJ·mol^{-1} in the gas phase versus 19.8 kJ·mol^{-1} in methanol. This process converts $[Pd(dhpe)(HC{\equiv}CH)(H)]^+$ ($\mathbf{2_{CB}}$) to the vinyl complex $[Pd(dhpe)(CH{=}CH_2)]^+$ ($\mathbf{3_{CB}}$). The opposite situation was found for the PH_3 case where $(\mathbf{2_{CM} \rightarrow 3_{CM}})\mathbf{TS}$ is 35.8 kJ·mol^{-1} in the gas phase but only 13.4 kJ·mol^{-1} in methanol. The potential energy values for all intermediates of the cationic cycle, containing both dhpe and PH_3, in the gas phase and continuum methanol are shown in Table 2.

When a specific methanol ligand is added to the coordination sphere of $\mathbf{1_{CM}}$ and$\mathbf{1_{CB}}$, local minima were found for a pair of

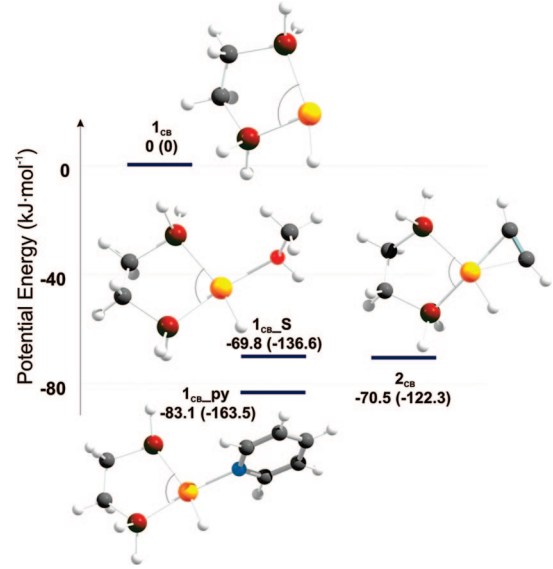

Figure 8. Optimized structures and relative potential energies of the palladium monohydride cation $\mathbf{1_{CB}}$, the methanol adduct $\mathbf{1_{CB}\_S}$, the pyridine adduct $\mathbf{1_{CB}\_py}$, and the η^2-alkyne complex $\mathbf{2_{CB}}$. The energies listed are in methanol (PCM model), with the values in parentheses corresponding to the gas phase values. Energies are relative to PdP_2H^+, HC≡CH, MeOH, and pyridine.

distorted square-planar complexes ($\mathbf{1_{CM}\_S}$ and $\mathbf{1_{CB}\_S}$). Solvent coordination stabilizes the system, with respect to the free ion and free methanol, in both cases by around 100 kJ·mol^{-1}. When the polarizable continuum model is used to simulate the effect of the "bulk" solvent in addition to an explicit methanol solvate, the corresponding energies fall by only ca. 70 kJ·mol^{-1} (Figure 8). The introduction of specific solvation is therefore important when considering the relative energies of species in the cationic system.

The structure of the pyridine adduct $Pd(dhpe)(H)(py)^+$ ($\mathbf{1_{CB}\_py}$) has also been calculated. These calculations reveal that the pyridine adduct is more stable than either the methanol or alkyne adducts ($\mathbf{2_{CB}}$) both in the gas phase and in the methanol continuum. This indicates that both pyridine and methanol can compete for binding to the metal with the alkyne substrate during catalysis. This observation is consistent with the experimental results where the corresponding monohydride complexes are only detected by PHIP NMR signals when pyridine is added to a methanol-based reaction mixture.

Coordination of the methanol or pyridine to 14-electron $\mathbf{3_{CB}}$ leads to the 16-electron adducts $[Pd(dhpe)(CH{=}CH_2)(L)]^+$ ($\mathbf{3_{CB}\_S}$ for L = methanol and $\mathbf{3_{CB}\_py}$ for L = pyridine; see Supporting Information for the structures). Now methanol coordination stabilizes the system by 54.1 kJ·mol^{-1}, while the

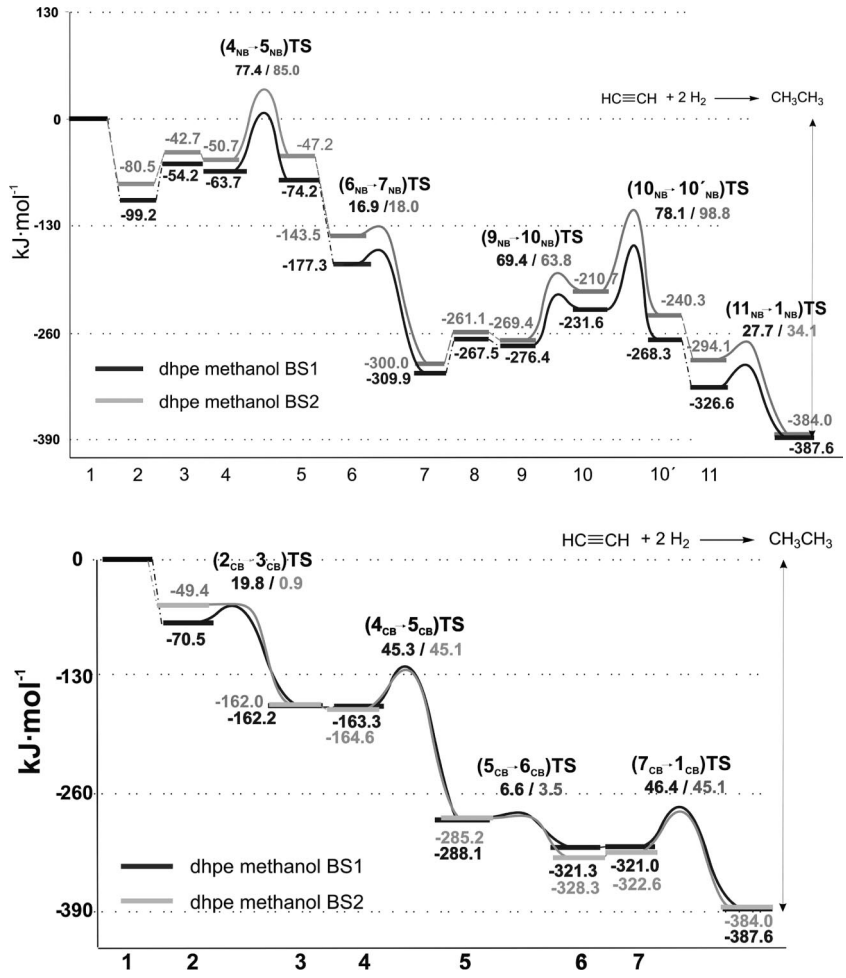

Figure 9. Energy profiles for the neutral (top) and cationic (bottom) mechanisms for the dhpe-based systems in methanol (polarizable continuum model) showing data obtained with BS1 and BS2 basis sets. Energies are relative to PdP_2 or PdP_2H^+, HC≡CH, and $2H_2$.

replacement of methanol by pyridine increases this energy gain to 77.3 kJ·mol^{-1}. The corresponding changes for the analogous PH_3-based complexes, **3$_{CM_S}$** and **3$_{CM_py}$**, in methanol are 87.0 and 107.7 kJ·mol^{-1}, respectively. The increased stability of the vinyl cations is also consistent with the experimental observations.

The methanol and pyridine adducts of **6$_{CB}$**, $[Pd(dhpe)(CH_2CH_3)(L)]^+$ (L = methanol or pyridine; **6$_{CB_S}$** and **6$_{CB_py}$**, respectively), have also been examined. They too are stabilized relative to the parent cation and free methanol or pyridine by similar amounts to those reported above (see Supporting Information). Experimentally, however, $[Pd(P_2)(CHPh\,CH_2Ph)](OTf)$ (P_2 = bcope or ^{t}bucope) prefers to interact in an *intra*molecular sense with the arene rather than with pyridine or methanol.

The stabilization of these intermediates by the solvent (methanol) or pyridine has significant catalytic implications, since these ligands compete with acetylene in the first step of the cation-based cycle. Indeed, the same is true for hydrogen addition to the vinyl species **3$_C$**, which has to react with dihydrogen in order for catalysis to proceed. When the stabilization of the vinyl species **3$_{CB}$** by methanol is considered (in a methanol continuum), the overall barrier to the formation of the η^2-alkene complex **5$_{CB}$** increases to 98.4 (and to 121.5 kJ·mol^{-1} when pyridine rather than methanol is displaced). This compares to a mere 44.2 kJ·mol^{-1} from **3$_{CB}$** itself. These data are consistent with the low signal intensities observed for the corresponding alkyl cations when pyridine-doped solvents are used.

Entropy Effects. Gibbs energy, enthalpy, and entropy data were introduced via appropriate vibrational analysis in the same way as already described for the neutral cycle. The results of this analysis are consistent with the deductions extrapolated from the potential energy profiles (see the Supporting Information).

Basis Set Dependence. The basis set dependence on the DFT results has been considered by recalculating the energy profiles of the dhpe-based systems using an extended basis set (BS2, see Computational Details) as recommended by one of the referees of the manuscript. In this case the metal is represented by the all-electron basis DZVP instead of the LANL2DZ core potential. The comparison between the energy profiles for the dhpe system in methanol obtained for both basis sets is shown in Figure 9 (tabulated data can be found in the Supporting Information). Now, for the dhpe-based cation in methanol there is virtually no barrier for hydride transfer to the alkyne ligand in **2$_{CB}$**. In this case (**2$_{CB}$** → **3$_{CB}$**)**TS** is 0.9 kJ·mol^{-1}, compared to 19.8 kJ·mol^{-1} as deduced using the BS1 basis set. Similarly, the transfer of the hydride ligand to the CH_2=CH_2 ligand of **5$_{CB}$** has a barrier, (**5$_{CB}$** → **6$_{CB}$**)**TS**, that is 3.1 kJ·mol^{-1} lower with the BS2 basis set. However, despite this and other small quantitative differences, the conclusions drawn from the new energy profiles do not differ from those deduced previously. These differences are illustrated in Figure 9.

Conclusions

Two possible reaction pathways for the palladium-bisphosphine-catalyzed semihydrogenation of akynes have been studied and compared with a number of experimental observations that were produced in a parallel experimental NMR investigation.[15] One mechanism is based on the neutral complex $Pd(0)P_2$, while the second involves a Pd(II) monohydride cation of the type PdP_2H^+.

Calculations and experimental observations support a reaction mechanism that is based on a cationic palladium monohydride precursor (palladium monohydrides were trapped experimentally as pyridine adducts). The energy barriers for the first hydride migration in $[Pd(P)_2(H)(\eta^2\text{-}HC{\equiv}CH)]^+$ (**2**$_{CM}$ or **2**$_{CB}$) to form the palladium vinyl $[Pd(P)_2(CH{=}CH_2)]^+$ (**3**$_{CM}$ or **3**$_{CB}$) are very low. This accounts for the observation of such complexes by PHIP NMR methods as methanol or pyridine adducts. The formation of the corresponding alkyls, $[Pd(P)_2(CH_2CH_3)]^+$ (**6**$_{CM}$ or **6**$_{CB}$) after H_2 addition to **3**$_C$ is also facile, and the alkyl palladium intermediates are stabilized by an agostic interaction (or by a stronger interaction with the phenyl ring of the $CHPhCH_2Ph$ ligand when a more realistic model is used). This observation also agrees with reported experimental data and explains why $[Pd(P)_2(CHPhCH_2Ph)]^+$ (P_2 = $2PEt_3$, bcope, or ^{t}bucope) is visible in solution rather than $[Pd(P)_2(L)(CHPhCH_2Ph)]^+$ (L = methanol or pyridine), which is predicted to be more stable by DFT. It also rationalizes why alkane formation, which requires H_2 coordination to $[Pd(P)_2(CHPhCH_2Ph)]^+$, is slow. Alkene isomerization, via β-H transfer, in $[Pd(P)_2(CH_2CH_3)]^+$ (**6**$_{CM}$ or **6**$_{CB}$) is predicted to compete effectively with H_2 addition and alkene liberation, again in good agreement with the earlier NMR and GC/MS observations. The mechanism for alkene isomerization, together with a low energy barrier for alkene rotation in the species $[Pd(P)_2(\eta^2\text{-}CH_2{=}CH_2)]^+$ (**5**$_{CM}$ and **5**$_{CB}$), demonstrates why hydrogen scrambling can place two hydrogen atoms from the same dihydrogen molecule into the same alkene (Scheme 3).[13–15]

This theoretical study has also pointed out that a neutral reaction cycle can be also operative, which ultimately places two dihydrogen molecules onto the metal center in a pairwise fashion. The detailed mechanism of the neutral cycle, however, reveals that phosphine loss is necessary to facilitate H_2 addition and alkyne semihydrogenation as revealed in Scheme 1. The calculations suggest that alkene isomerization should be very slow in the neutral system as a result of the high energy barriers found for alkyl palladium hydride formation. What is more, alkane elimination from this bisphosphine alkyl palladium hydride, as modeled by **11**$_N$, should be facile. However, as a consequence of the high energy barriers involved in its formation, the production of substantial amounts of the alkane are not predicted. The theoretical results obtained for the neutral catalytic cycle do not match well with the observations made in the parallel experimental study. Examples of such reactions can, however, be found in the literature for related systems.[7]

When a continuum solvent model was introduced into the calculations, no significant changes in the energy profiles for the associated reactions were found in either the neutral or the preferred cationic mechanisms. The experimental observations clearly indicate, however, that there is much higher catalyst activity in methanol rather than dichloromethane. This enables us to conclude that the major role of the solvent in the real reaction is to facilitate the generation of higher concentrations of the cationic palladium monohydrides necessary for catalysis.

While the results reported here are specific to alkyne hydrogenations, the individual steps featured in the two reaction cycles are common to alkene hydroformylation, CO−alkene copolymerization, and alkene polymerization. The results of this study will therefore contribute to improving our understanding of such reactions.

Acknowledgment. We are grateful for EU funding under the HYDROCHEM network (contract HPRN-CT-2002-00176). Financial support from the Spanish MEC (Project Consolider Ingenio 2010 CSD2007-00006) is also acknowledged. The use of computational facilities of the Centre de Supercomputació de Catalunya (CESCA) is gratefully appreciated.

Supporting Information Available: Additional energy profiles and tables. Figures, *xyz* coordinates, and absolute energies (hartree) for intermediate complexes and transition states. This material is available free of charge via the Internet at http://pubs.acs.org.

OM700307C